J. Cent. South Univ. (2020) 27: 554−565
DOI: https://doi.org/10.1007/s11771-020-4316-z

Springer

Freeze-thaw damage mechanism of elastic modulus of soil-rock mixtures at different confining pressures

ZHOU Zhong(周中)[1], LIU Zhuang-zhuang(刘撞撞)[1], YANG Hao(杨豪)[1, 2], GAO Wen-yuan(高文渊)[1], ZHANG Cheng-cheng(张称呈)[1]

1. School of Civil Engineering, Central South University, Changsha 410075, China;
2. Department of Architecture and Civil Engineering, City University of Hong Kong, Hong Kong, China

Abstract: As a frequently-used roadbed filler, soil-rock mixture is often in the environment of freeze-thaw cycles and different confining pressures. In order to study the freeze-thaw damage mechanism of elastic modulus of soil-rock mixtures at different confining pressures, the concept of meso-interfacial freeze-thaw damage coefficient is put forward and the meso-interfacial damage phenomenon of soil-rock mixtures caused by the freeze-thaw cycle environment is concerned; a double-inclusion embedded model for elastic modulus of soil-rock mixtures in freezing-thawing cycle is proposed. A large triaxial test was performed and the influences of confining pressure and experimental factors on elastic modulus of soil-rock mixtures were obtained, and then the accuracy of the double-inclusion embedded model to predict the elastic modulus of soil-rock mixtures in freezing-thawing cycle is verified. Experiment results showed that as to soil-rock mixtures, with the increase of confining pressure, the elastic modulus increases approximately linearly. The most crucial factors to affect the elastic modulus are rock content and compaction degree at the same confining pressure; the elastic modulus increases with the increase of rock content and compactness; as the number of freeze-thaw cycles increases, the freeze-thaw damage coefficient of meso-structural interface and the elastic modulus decrease.

Key words: soil-rock mixtures; confining pressure; freeze-thaw cycle; elastic modulus; damage coefficient

Cite this article as: ZHOU Zhong, LIU Zhuang-zhuang, YANG Hao, GAO Wen-yuan, ZHANG Cheng-cheng. Freeze-thaw damage mechanism of elastic modulus of soil-rock mixtures at different confining pressures [J]. Journal of Central South University, 2020, 27(2): 554−565. DOI: https://doi.org/10.1007/s11771-020-4316-z.

1 Introduction

The granulometric composition of soil-rock mixtures is extremely dispersive. The coarse granules, such as rubbles and gravels, skeletonize the soil-rock mixtures; while the fine particles, such as sands and clays, fill the void of the skeleton. So, the mechanic property of soil-rock mixtures depends on the combined effect of coarse granules and fine particles [1]. Soil-rock mixture is a common backfilling geo-material in civil engineering, and it is often applied to the construction of riverbanks, roadbeds, dams, port yards, and foundations, and widely distributed in seasonally frozen-ground region [2].

Elastic modulus of soil-rock mixtures can be used to predict the landslide mechanism of accumulation slope and design roadbed padding made of coarse soils [3]. However, elastic characteristic research on soil-rock mixtures is still based on engineering experience. The elastic modulus of soil-rock mixtures is determined by experimental methods. ZHANG et al [4] and LI et al [5] used the indoor shear creep test to study the long-term strength of soil-rock mixtures in the

Foundation item: Project(50908234) supported by the National Natural Science Foundation of China
Received date: 2019-02-26; **Accepted date:** 2019-05-21
Corresponding author: YANG Hao, Research Assistant; Tel: +86-18900799837; E-mail: 1204952285@qq.com; ORCID: 0000-0002-4204-7814

Chengdu area of China, but this method is time-consuming, expensive, and can only determine the elastic modulus of soil-rock mixtures at some certain area. Some scholars studied the deformation characteristics, such as small deformation and non-collapsibility of soil-rock mixtures from dams by the moisture-density test. The empirical equation methods work under some certain test conditions [6−9]. If out of the certain test conditions of empirical equation methods, the prediction error will be quite big and the result will be misleading [10−12]. XING et al [13] analyzed the destructive behavior of soil-rock mixtures with different rock content after the freeze-thaw cycle through large indoor three-axis experiments, but the theoretical calculation model of the characteristics of soil-rock mixture under freeze-thaw cycle is not obtained. ZHOU et al [14] carried out a microscopic simulation of soil-rock mixture using PFC^{3D}, and analyzed the influence of freeze-thaw cycle on the intergranular strength of soil-rock. However, both test methods and empirical equation methods can not accurately reflect the microscopic mechanics of soil-rock mixtures [15, 16]. As a result, in order to make sure that the design of soil-rock mixtures is real effective and safe, it is necessary to establish suitable mechanical models to predict the elastic properties of the earth-rock mixture in the complex natural environment.

MA et al [17] studied the equivalent elastic modulus of sandy pebble soils while without concerning the Poisson ratio in the prediction model. YANG et al [18] proposed two models for the prediction of the elastic modulus of soil-rock mixtures under freezing state, but the soil-rock mixtures in freezing-thawing cycle have not yet been studied. KANG et al [19] studied the mechanical properties of muddy sandy soil under freezing-thawing cycles. WANG et al [20] studied and analyzed the properties of powdered soil mechanics through the process of freezing and thawing cycle through indoor three-axis test. ROUSTAEI et al [21] carried out an experimental study on the mechanical parameters of fiber-reinforced fine grain soil after the effect of freeze-thaw circulation. XU et al [22] designed laboratory studies on energy dissipation and injury studies on frozen loess during deformation. JAMSHIDI et al [23] studied the hydraulic strength properties of different types of soil-cement under freezing-thawing cycles. JAMSHIDI et al [24] also studied the effect of freeze-thaw cycles on the performance and microstructure of cement-treated soils. ROSA et al [25] conducted laboratory studies on the freeze-thaw properties of fly ash stabilizing materials and recycled road materials. GEER et al [26] used image data obtained from scanning acoustic microscopes to estimate the effective elastic modulus of geological materials.

The soil-rock mixtures are widely distributed in seasonally frozen-ground region [27]. With the development of construction in this region, the research on soil-rock mixtures under freeze–thaw cycle action should be comprehensively studied by the laboratory tests and the theoretical analysis. So, building the mechanical model for soil-rock mixtures under freeze-thaw cycle is very essential because of the basic universality of theoretical analysis [28, 29].

It is important to study the elastic modulus of soil-rock mixtures at different confining pressures, because the geo-materials always work at different confining pressures in engineering. The large-scale of triaxial test apparatus is adopted to test the elastic modulus of soil-rock mixtures at different confining pressures. Then based on the existing theory [18], a double-inclusion embedded model is set up to calculate the elastic modulus of soil-rock mixtures in freeze-thaw cycle. Finally, the experimental results verified the calculation model of the elastic modulus of soil-rock mixture.

2 Experiment analysis

The experiment was based on the test platform of the National Engineering Laboratory for High Speed Railway Construction. The large-scale of static triaxial test apparatus was adopted to test elastic modulus of the soil-rock mixtures at different confining pressures.

In this paper, the mechanical damage effect of soil and rock mixture under freezing-thawing environment is studied by orthogonal test. The factors include rock content (A), compaction degree (B), water content (C), number of freeze-thaw cycles (D), freezing temperature (E), and each factor has four different levels. The factors and levels of the designed orthogonal test are shown in

Table 1. The scheme of orthogonal designed large-scale triaxial test is shown in Table 2.

Table 1 Factors and levels of designed orthogonal test

Level	Factor				
	A	B	C	D	E
1	35%	87%	2%	0	−2 °C
2	45%	90%	4%	3	−5 °C
3	55%	92%	6%	6	−8 °C
4	65%	95%	8%	10	−11 °C

Through indoor large-scale triaxial experiment, a total of 64 stress−strain curves of 16 groups of soil-rock mixture samples under different confining pressure and five factors were obtained. The secant modulus of axial strain varying from zone to a third of the peak strain corresponding to the maximum static strength is regarded as the elastic modulus of soil-rock mixtures. The test results of elastic modulus of each specimen of soil-rock mixtures under different conditions are summarized in Table 2.

Under different confining pressure, the elastic modulus of the specimen changes greatly. With the increase of confining pressure, the elastic modulus of the test piece increases. The effect of orthogonal design factors on elastic modulus is analyzed by polar analysis and anovaise method of orthogonal test.

Sample SY14 (The test results and the values of influencing factors are shown in Table 2) is taken as an example to draw stress−strain curve, as shown in Figure 1.

It can be concluded from Figure 1 that the soil-rock mixture is a material conforming to the binary medium model [30], and consists of soil-covered macadam structure (the bonding element) and interface between structural pores and inclusions (the frictional element). When the confining pressure is low, as the deviatoric stress increases, the soil-covered macadam structure is gradually crushed, forming more interface between structural pores and inclusions, which causes more bonding elements to be converted into frictional elements. The deformation modulus of the friction element is lower than the deformation modulus of the bonding element at low confining pressure, so that the pressure difference formed by the transformation of the bonding element into the friction element is larger, and the soil-rock mixture exhibits obvious strain-softening; as the confining pressure increases, the deformation modulus of the frictional element increases, and the pressure difference formed by the transition from bonding element to friction element decreases, which weakens the strain-softening property of soil-rock

Table 2 Orthogonal designed test scheme and results of elastic modulus

Test No.	Factor					Elastic modulus/MPa			
	A	B	C	D	E	50 kPa	100 kPa	200 kPa	300 kPa
SY1	35%	87%	2%	0	−2 °C	6.61	8.64	12.22	15.43
SY2	35%	90%	4%	3	−5 °C	6.58	8.67	12.09	15.47
SY3	35%	92%	6%	6	−8 °C	6.89	9.21	13.47	17.41
SY4	35%	95%	8%	10	−11 °C	6.39	9.67	12.37	16.41
SY5	45%	87%	4%	6	−11 °C	7.55	9.52	13.17	16.33
SY6	45%	90%	2%	10	−8 °C	7.48	9.61	13.01	16.37
SY7	45%	92%	8%	0	−5 °C	8.13	10.54	14.84	18.71
SY8	45%	95%	6%	3	−2 °C	7.66	10.92	13.71	17.71
SY9	55%	87%	6%	10	−5 °C	8.31	10.27	14.02	17.11
SY10	55%	90%	8%	6	−2 °C	8.80	11.01	14.22	17.67
SY11	55%	92%	2%	3	−11 °C	9.57	12.04	16.27	20.11
SY12	55%	95%	4%	0	−8 °C	9.42	12.76	15.53	19.61
SY13	65%	87%	8%	3	−8 °C	11.10	13.15	16.75	19.95
SY14	65%	90%	6%	0	−11 °C	11.85	14.05	17.20	20.70
SY15	65%	92%	4%	10	−2 °C	10.70	13.15	17.35	21.25
SY16	65%	95%	2%	6	−5 °C	11.25	14.55	17.35	21.45

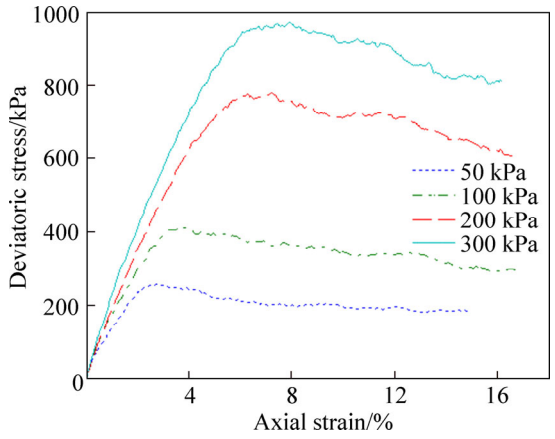

Figure 1 Stress−strain relationship of soil-rock mixture sample SY14 under different test conditions

mixture under high confining pressure. For the same specimen, the increasing of confining pressure resulted in increased elastic modulus, which shows that the restraint caused by high confining pressure is significant. In addition, the impacts of the orthogonal designed factors on the elastic modulus need to be analyzed by means of range analysis and variance analysis.

2.1 Analysis of relationship between elastic modulus and confining pressure

According to the triaxial test results, the relationship between elastic modulus and confining pressure of each specimen is shown in Figure 2.

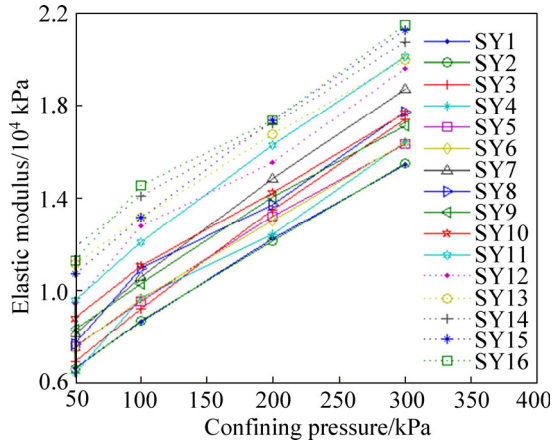

Figure 2 Relation curve of elastic modulus and confining pressure

By surveying the influence law between elastic modulus and confining pressure, the elastic modulus increases with the increase of confining pressure, and the trend presents nearly linear positive correlation. Then the relation equation of linear positive correlation between confining pressure and elastic modulus is assumed in this study:

$$E = m\sigma_3 + n \tag{1}$$

where n is the elastic modulus of the soil-rock mixture without confining pressure; m is the confining pressure coefficient, which is related to the mechanical properties of the soil-rock mixtures. According to the test data of σ_3 and E, as shown in Table 2, m and n of each specimen can be fitted by Eq. (1), as summarized in Table 3.

Table 3 Coefficient summary of relation between elastic modulus and confining pressure

Test No.	m	n/kPa
SY1	35.2	5012.7
SY2	35.2	4980.8
SY3	42.0	4922.2
SY4	37.9	5053.7
SY5	35.1	5936.3
SY6	35.2	5903.6
SY7	42.2	6199.2
SY8	38.1	6308.5
SY9	35.3	6691.5
SY10	34.8	7263.4
SY11	41.9	7684.1
SY12	38.5	8065.8
SY13	35.3	9505.9
SY14	35.0	10309.0
SY15	41.9	8795.8
SY16	38.6	9870.3

The range of m is 35−43. By calculating the average of the test piece confining pressure coefficient m under the same rock content, the relationship between rock content and m can be obtained as shown in Table 4.

The relation curve between confining pressure coefficient m and rock content is shown in Figure 3.

Table 4 Relation between rock content and coefficient m

Rock content/%	m
35	37.58
45	37.65
55	37.63
65	37.70

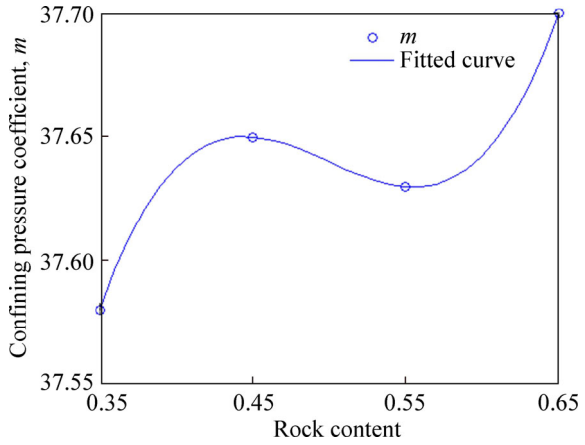

Figure 3 Relational graph of confining pressure coefficient m and rock content

It can be seen that the confining pressure coefficient increases with the increase of rock content.

The polynomial function fitted by the confining pressure coefficient m and the rock content C_R is shown as:

$$m = 30C_R^3 - 45C_R^2 + 22.225C_R + 34.0275 \quad (2)$$

According to the experimental results, it can be found that, compared with other geotechnical materials, the elastic modulus of soil-rock mixtures is significantly affected by confining pressure changes. The reason is that the lateral deformation of relatively loose materials such as soil-rock mixture is greatly affected by the restraint effect under the confining pressure. The deformation modulus of the friction element is lower than the deformation modulus of the bonding element at low confining pressure, so that the pressure difference formed by the transformation of the bonding element into the friction element is larger, and the soil-rock mixture exhibits obvious strain-softening; as the confining pressure increases, the deformation modulus of the frictional element increases, and the pressure difference formed by the transition from bonding element to friction element decreases, which weakens the strain-softening property of soil-rock mixture under high confining pressure. For the same sample, the elastic modulus increases due to the increase of confining pressure, indicating that the constraint effect caused by high confining pressure on the specimen is significant. Moreover, different confining pressures lead to different constraint strengths, which leads to the change of elastic modulus of earth-rock mixture with the change of confining pressures.

2.2 Effect of experimental factors on elastic modulus

By calculating the value range of the five factors, the influence degree of each test factor on the elastic modulus was obtained, as shown in Table 5, and then the relational graph of them was got as shown in Figure 4. Then the influence degree of various factors on the elastic modulus of soil-rock mixtures was analyzed by variance analysis method of variance experiment.

According to the data in Table 5, it can be found that the differences in the experimental results of different groups are caused by the level of experimental factors, rather than errors. And The influence degree order of factors at different confining pressure is obtained. It can be seen that for soil-rock mixtures materials, rock content and compaction degree have the greatest influence on its elastic modulus, and it increases with the increase of rock content and compacting degree. Followed by the number of freezing-thawing cycles, with more freezing-thawing cycles, the elastic modulus of soil-rock mixtures become smaller. The influence of water content and freezing temperature on the elastic modulus of soil-rock mixture is small. Therefore, in the application of soil-rock mixture, the elastic modulus of soil-rock mixture can be effectively controlled by adjusting the stone content and density.

3 Application of freeze-thaw damage model

The environment of freeze-thaw cycle brings some damage effects to the interfacial layer of particles of soil-rock mixtures [31, 32]. There are lots of interface voids between rock aggregates and soils due to the loose and stochastic properties of soils [33]. The physical change of pore water in the interface voids is subjected to the freeze-thaw cycle environment, which will lead to the change of mechanics properties for interface layer between rock aggregates and soils. Owing to the volume expansion of pore water in the process from liquid to solid, the interface layer of soil-rock mixtures under freeze-thaw cycle will be damaged by the inflated deformation phenomenon of pore water [34, 35], which will affect the mechanical properties of soil-rock mixtures. YANG et al [18] established a two-layer embedded model of single inclusion

Table 5 Analysis of variance experiment results

Confining pressure/kPa	Influence factor	Level 1	Level 2	Level 3	Level 4	Range	Variance analysis				
							Dev-Sq	DOF	*F*-ratio	*P*-value	Significance
50	A	6.62	7.71	9.03	11.23	4.61	47.18	3	725.86	<0.01	***
	B	8.39	8.68	8.82	8.68	0.43	0.39	3	6.00	<0.10	*
	C	8.73	8.56	8.68	8.61	0.16	0.07	3	1.00	>0.10	
	D	9	8.73	8.62	8.22	0.78	1.26	3	19.43	<0.05	**
	E	8.44	8.57	8.72	8.84	0.4	0.36	3	5.60	<0.05	*
	Error						0.07	3			
100	A	9.05	10.15	11.52	13.73	4.68	48.75	3	696.39	<0.01	***
	B	10.4	10.84	11.24	11.98	1.58	5.40	3	77.19	<0.01	***
	C	11.21	11.03	11.11	11.09	0.19	0.07	3	1.00	>0.10	
	D	11.5	11.2	11.07	10.68	0.82	1.39	3	19.89	<0.05	**
	E	10.93	11.01	11.18	11.32	0.39	0.37	3	5.27	>0.10	
	Error						0.07	3			
200	A	12.54	13.68	15.01	17.16	4.63	47.32	3	591.51	<0.01	***
	B	14.04	14.13	15.48	14.74	1.44	5.33	3	66.65	<0.01	***
	C	14.71	14.54	14.6	14.55	0.18	0.08	3	1.00	>0.10	
	D	14.95	14.71	14.55	14.19	0.76	1.22	3	15.21	<0.05	**
	E	14.38	14.58	14.69	14.75	0.38	0.33	3	4.13	>0.10	
	Error						0.08	3			
300	A	16.18	17.28	18.63	20.84	4.66	48.24	3	660.82	<0.01	***
	B	17.21	17.55	19.37	18.8	2.17	12.51	3	171.43	<0.01	***
	C	18.34	18.17	18.23	18.19	0.18	0.07	3	1.00	>0.1	
	D	18.61	18.31	18.22	17.79	0.83	1.40	3	19.23	<0.05	**
	E	18.02	18.19	18.34	18.39	0.37	0.34	3	4.60	>0.1	
	Error						0.07	3			

composite material to obtain the elastic modulus of soil-rock mixture (can be abbreviated as S-RM) considering rock wrapped by soil in the mesoscopic structure of soil-rock mixture at normal temperature, and established a three-layer embedded model of double inclusion composite material and multistep multiphase micromechanics model to obtain the elastic modulus of a frozen soil-rock mixture by giving an interface ice interlayer attached between the soil and rock interface in the mesoscopic structure of soil-rock mixture at freezing temperature. But the soil-rock mixtures in freeze-thaw cycle has not yet been studied.

As to the soil-rock mixtures in the freeze-thaw cycle, considering the interfacial layer between the rock aggregates and the soils [36, 37], it can be taken as a three-phase composite which is composed of rock aggregates, interfacial layer, and soils. Then based on the existing theory [18], a double-inclusion embedded model is set up to calculate the elastic modulus of soil-rock mixtures in freeze-thaw cycle (can be abbreviated as FS-RM). In order to simplify the meso-structure, the diagram of circular double-inclusion embedded model is established, as shown in Figure 5.

The “mechanics method of decomposing the whole into several parts” is employed to simplify the double-inclusion embedded model. Firstly, take the rock aggregates wrapped by the interfacial layer as an independent research object, which is a single-inclusion model called transition-inclusion body. So, the elastic modulus of the transition-inclusion body can be solved by the former single-inclusion embedded prediction model. Secondly, take the transition-inclusion body wrapped by the soils as an independent research object, which is a single-inclusion model called final-inclusion body. So, the elastic modulus of the

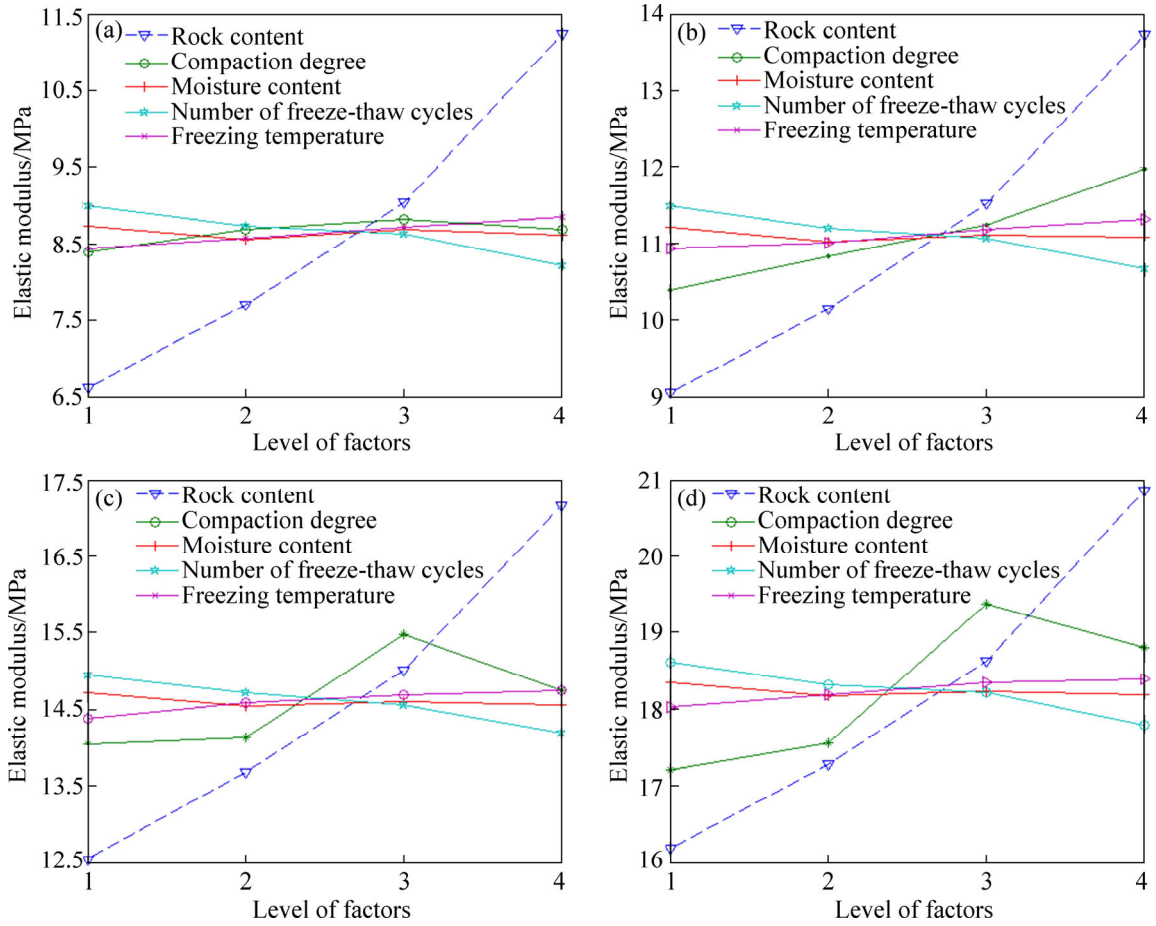

Figure 4 Relationship between elastic modulus under different confining pressures and various experimental factors: (a) 50 kPa; (b) 100 kPa; (c) 200 kPa; (d) 300 kPa

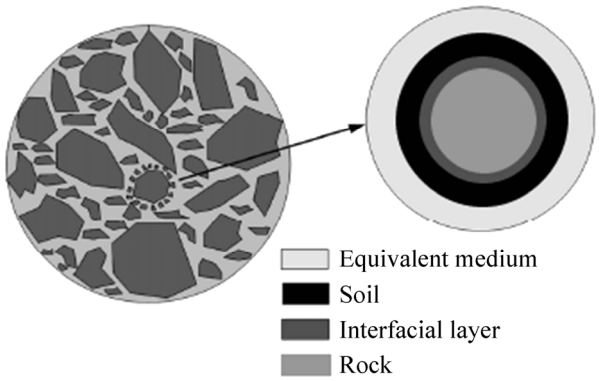

Figure 5 Meso-structure of soil-rock mixtures considering interface effect

final-inclusion body can be solved by the former single-inclusion embedded prediction model. That is, the elastic modulus of soil-rock mixtures after freeze-thaw cycle can be solved after twice using the single-inclusion embedded prediction model.

The interfacial layer of soil-rock mixtures under normal state was not considered in the single-inclusion embedded prediction model before. So, the double-inclusion embedded prediction model for soil-rock mixtures after freeze-thaw cycle is also suitable for soil-rock mixtures under normal state.

In order to estimate the damaging degree of interfacial layer, the concept about freeze-thaw damage coefficient of meso-structural interfacial layer is put forward in this study. The formula of damage coefficient δ is defined as:

$$\delta = \frac{\delta_n}{\delta_0} \times 100\% \tag{3}$$

where δ_0 is the freeze-thaw damage coefficient of soil-rock mixtures after non-freeze-thaw cycle; δ_n is the freeze-thaw damage coefficient of soil-rock mixtures after n freeze-thaw cycles.

Then the calculation model of the elastic modulus of soil-rock mixture is verified and compared with the experimental results.

3.1 S-RM under normal environment

Before applying the embedded model of soil-rock mixtures under normal state (can be abbreviated as S-RM) [12], the volume fraction of

each phase, such as soils, rocks, structural void, should be determined by the three-phase diagram of soil-rock mixtures, as shown in Table 6. Among the 16 sets of specimens, four specimens (SY1, SY7, SY12, and SY14) are the S-RM without freeze-thaw cycle.

Table 6 Volume fraction of each phase in each specimen

Test No.	Rock content/%	Number of freeze-thaw cycles	Volume fraction/%		
			Soils	Rocks	Structural void
SY1	35	0	65.2	31.4	3.4
SY2	35	3	65.5	32.1	2.4
SY3	35	6	65.7	32.6	1.7
SY4	35	10	66.1	33.2	0.7
SY5	45	6	55.4	40.3	4.3
SY6	45	10	55.7	41.1	3.2
SY7	45	0	55.9	41.4	2.7
SY8	45	3	56.2	42.1	1.7
SY9	55	10	44.9	49.5	5.6
SY10	55	6	45.3	49.8	4.9
SY11	55	3	45.8	50.2	4.0
SY12	55	0	46.2	50.9	2.9
SY13	65	3	35.1	59.1	5.8
SY14	65	0	35.5	59.5	5.0
SY15	65	10	35.8	59.7	4.5
SY16	65	6	36.2	60.4	3.4

The elastic modulus of soil is 2.62 MPa and Poisson ratio is 0.4. The elastic modulus of rock is 40 GPa and Poisson ratio is 0.2. The structural void was formed by an incomplete parcel by soils in the interfacial layer between soils and rock aggregates. Therefore, structural void and soils coexist in the contact surface of the rock aggregates. The equivalent elastic property of the interfacial layer should be between soils and structural void, and it is proposed as α times the elastic property of soils. The α is called structural coefficient of interfacial layer, which is figured up by back-analysis method using laboratory test data.

The single-inclusion embedded model and the double-inclusion embedded model are used to calculate the elastic modulus of S-RM. The test data n can be calculated by Eqs. (1) and (2). The calculation results are shown in Table 7.

The prediction value of double-inclusion embedded model is less than the value of single-inclusion embedded model in general. That is because the structural void plays a weakening effect in the elastic modulus of soil-rock mixtures. After considering the weakening effect of interfacial structural void, the difference between the prediction value of double-inclusion embedded model and the test result is quite small.

The relation curve between rock content and elastic modulus of S-RM is shown in Figure 6. The elastic modulus of S-RM increases with the increase of rock content, especially during the range of 45%−55%.

3.2 FS-RM under freeze-thaw cycle environment

The structural void of soil-rock mixtures after freeze-thaw cycle (can be abbreviated as FS-RM) is hypothesized the same as the structural void of S-RM. The volume fraction of each phase of each specimen is shown in Table 6. Among the 16 sets of specimens, 12 sets of specimens (SY2 to SY16) are the FS-RM with several freeze-thaw cycles.

The double-inclusion embedded model is used to calculate the elastic modulus of FS-RM. The test data n can be calculated by Eqs. (1)−(2). The freeze-thaw damage coefficient δ is calculated by the back-analysis method. The results are shown in Table 8.

With the increase of the number of freeze-thaw cycles, the elastic modulus of soil-rock mixtures was gradually reduced. The elastic modulus of soil-rock mixtures after freeze-thaw cycle increases with the increase of rock content.

Table 7 Elastic modulus of S-RM by two proposed models and laboratory test

Test No.	Rock content/%	Number of freeze-thaw cycles	S–RM		Laboratory test value, n	Structural coefficient, α
			Single-inclusion model	Double-inclusion model		
SY1	35%	0	4.86	5.01	5.01	0.5
SY7	45%	0	6.25	6.25	6.20	0.5
SY12	55%	0	8.29	8.03	8.07	0.5
SY14	65%	0	11.67	10.17	10.31	0.5

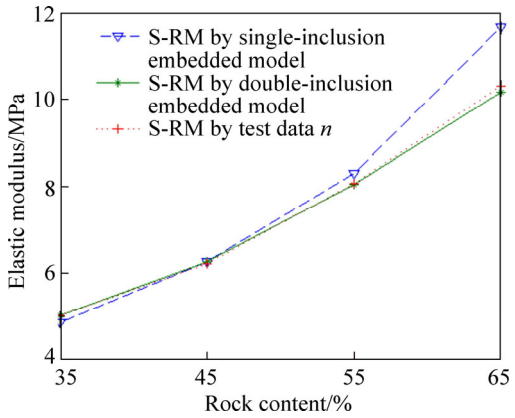

Figure 6 Relation curve between rock content and elastic modulus of S-RM

Table 8 Elastic modulus of FS-RM by proposed model and laboratory test

Test No.	Rock content/%	Number of freeze-thaw cycles	S–RM (Double-inclusion model)	Laboratory test value n	Freeze-thaw damage coefficient, δ
SY2	35	3	4.98	4.98	0.73
SY3	35	6	4.97	4.92	0.55
SY4	35	10	4.98	5.05	0.43
SY5	45	6	5.84	5.94	0.59
SY6	45	10	5.85	5.90	0.46
SY8	45	3	6.25	6.31	0.77
SY9	55	10	6.64	6.69	0.50
SY10	55	6	7.15	7.26	0.61
SY11	55	3	7.68	7.68	0.81
SY13	65	3	9.52	9.51	0.84
SY15	65	10	8.78	8.80	0.52
SY16	65	6	9.84	9.87	0.64

Table 9 shows the mean value of the freeze-thaw damage coefficient δ of different specimens under the same number of freeze-thaw cycles. With the increase of the number of freeze- thaw cycles, the freeze-thaw damage coefficient decreases gradually.

Table 9 Mean value of freeze-thaw damage coefficient δ of different specimens under same number of freeze-thaw cycles

Number of freeze-thaw cycles	Mean value of freeze-thaw damage coefficient δ
0	1.00
3	0.79
6	0.60
10	0.48

Figure 7 shows the relation curves of the mean value of the freeze-thaw damage coefficient with different numbers of freeze-thaw cycles. When the number of freeze-thaw cycle is zero, the freeze-thaw damage coefficient is one. When the number of freeze-thaw cycles is less than 6, with increasing of the number of freeze-thaw cycles, the freeze-thaw damage coefficient of meso-structural interface decreases rapidly. When the number of freeze-thaw cycles is more than 6, with increasing of the number of freeze-thaw cycles, the freeze-thaw damage coefficient of meso- structural interface decreases slowly.

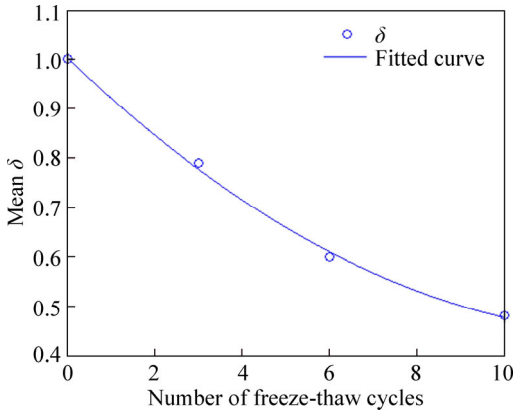

Figure 7 Relation curves of mean value of freeze-thaw damage coefficient with different numbers of freeze-thaw cycles

The empirical formula of the mean value of the freeze-thaw damage coefficient with different numbers of freeze-thaw cycles is fitted as:

$$\delta = 0.0032n^2 - 0.085n + 1.0042 \quad (4)$$

3.3 Accuracy assessment of proposed model

The relative error of elastic modulus between the test data and the proposed models is shown in Table 10. The accuracy of the proposed models can be verified by the lager-scale triaxial test designed by the orthogonal experiment method. The maximum relative error of the single-inclusion embedded model is 13.21%, while the maximum relative error of the double-inclusion embedded model is 1.59%.

4 Conclusions

1) Based on existing theories, the freeze-thaw damage coefficient of interfacial layer of soil-rock mixtures is put forward, and then the double-

Table 10 Relative error of elastic modulus between proposed models and test data

Test No.	Rock content/%	Number of freeze-thaw cycles	Relative error of elastic modulus/%		
			S–RM (Single-inclusion embedded model)	S–RM (Double-inclusion embedded model)	FS–RM (Double-inclusion embedded model)
SY1	35	0	−3.00	−0.02	—
SY2	35	3	—	—	0.06
SY3	35	6	—	—	0.98
SY4	35	10	—	—	−1.54
SY5	45	6	—	—	−1.59
SY6	45	10	—	—	−0.98
SY7	45	0	0.75	0.75	—
SY8	45	3	—	—	−1.00
SY9	55	10	—	—	−0.78
SY10	55	6	—	—	−1.51
SY11	55	3	—	—	−0.05
SY12	55	0	2.83	−0.48	—
SY13	65	3	—	—	0.19
SY14	65	0	13.21	−1.35	—
SY15	65	10	—	—	−0.21
SY16	65	6	—	—	−0.33

inclusion embedded model is established to predict the elastic modulus of soil-rock mixtures under freeze-thaw cycle environment. The accuracy of the proposed model is verified by the lager-scale triaxial test designed by the orthogonal experiment method. The maximum relative error of the single-inclusion embedded model is 13.21%, while the maximum relative error of the double-inclusion embedded model is only 1.59%.

2) The soil-rock mixture is quite sensitive to the confining pressure, and shows obvious strain softening property under low confining pressure. With the increase of confining pressure, the strain softening property of soil-rock mixture decreases continuously. The elastic modulus of soil-rock mixtures increases with the increase of confining pressure, and the trend presents nearly linear positive correlation, and the positive correlation coefficient is mainly related to the rock content.

3) Rock content and compaction degree have the greatest influence on elastic modulus of soil-rock mixtures, and it increases with the increase of rock content and compacting degree. Followed by the number of freezing-thawing cycles, with more freezing-thawing cycles, the elastic modulus of soil-rock mixtures become smaller. The influence of water content and freezing temperature on the elastic modulus of soil-rock mixture is small.

4) When the number of freeze-thaw cycles is less than six, with the increase of the number of freeze-thaw cycles, the freeze-thaw damage coefficient of meso-structural interface decreases rapidly. After more than six freezing-thawing cycles, with increasing of the number of freeze-thaw cycles, the freeze-thaw damage coefficient of meso-structural interface decreases slowly.

References

[1] AN R J, HU R L, XU W J. Some geomechanical properties of soil-rock mixtures in the Hutiao Gorge area, China [J]. Géotechnique, 2007, 57(3): 255−264.

[2] ZHOU Z, YANG H, WAN Z H, LIU B C. Computational model for electrical resistivity of soil–rock mixtures [J]. Journal of Materials in Civil Engineering, 2016, 28(8): 06016009.

[3] BOURKAS G, PRASSIANAKIS I, KYTOPOULOS V, SIDERIDIS E, YOUNIS C. Estimation of elastic moduli of particulate composite by new models and comparison with moduli measured by tension, dynamic, and ultrasonic tests [J]. Advances in Materials Science and Engineering, 2010,

2010: 891824.

[4] ZHANG D B, LIU Z Z, ZHANG J H. A new failure mechanism for deep cavity and upper bound solution of supporting pressure [J]. Journal of Central South University, 2017, 24(9): 2082−2091.

[5] LI H, SHI S L, LU J X, YE Q, LU Y, ZHU X N. Pore structure and multifractal analysis of coal subjected to microwave heating [J]. Powder Technology, 2019, 346: 97−108.

[6] CALDEIRA M S, MARIA L, BRITO A. Use of soil-rock mixtures in dam construction [J]. Journal of Construction Engineering and Management, 2014, 140(8): 04014030.

[7] YANG X L, CHEN J H. Factor of safety of geosynthetic-reinforced slope in unsaturated soils [J]. International Journal of Geomechanics, 2019, 19(6): 04019041.

[8] LI Z W, YANG X L, LI T Z. Static and seismic stability assessment of 3D slopes with Cracks [J]. Engineering Geology, 2020, 265: 105450.

[9] ZHANG D B, ZHANG B. Stability analysis of the pressurized 3D tunnel face in anisotropic and nonhomogeneous soils [J]. International Journal of Geome Chanics, 2020, 20(4): 04020018.

[10] QI J L, MA W, SONG C. Influence of freeze–thaw on engineering properties of a salty soil [J]. Cold Regions Science and Technology, 2008, 53(3): 397−404.

[11] NISHIMURA S, GENS A, OLIVELLA S, JARDINE R J. THM-coupled finite element analysis of frozen soil: Formulation and application [J]. Géotechnique, 2009, 59(3): 159−171.

[12] LI T Z, YANG X L. Stability of plane strain tunnel headings in soils with tensile strength cut-off [J]. Tunnelling and Underground Space Technology, 2020, 95: 103138.

[13] XING K, ZHOU Z, YANG H, LIU B C. Macro–meso freeze–thaw damage mechanism of soil–rock mixtures with different rock contents [J]. International Journal of Pavement Engineering, 2020, 21(1): 9−19.

[14] ZHOU Z, XING K, YANG H, WANG H. Damage mechanism of soil-rock mixture after freeze-thaw cycles [J]. Journal of Central South University, 2019, 26(1): 13−24.

[15] SHOOP S, AFFLECK R, HAEHNEL R, JANOO V. Mechanical behavior modeling of thaw-weakened soil [J]. Cold Regions Science and Technology, 2008, 52(2): 191−206.

[16] ZHONG J H, YANG X L. Kinematic stability of tunnel face in non-uniform soils [J]. KSCE Journal of Civil Engineering, 2020, 24(2): 670−681.

[17] MA H, GAO M Z, ZHANG J K, YU Q F. Theoretical model developed for equivalent elastic modulus estimation of cobblestone-soil matrix [J]. Rock and soil Mechanics, 2011, 32(12): 3642−3646.

[18] YANG H, ZHOU Z, WANG X C, ZHANG Q F. Elastic modulus calculation model of a soil–rock mixture at normal or freezing temperature based on micromechanics approach [J]. Advances in Materials Science and Engineering, 2015, 2015: 576080.

[19] KANG M, LEE J S. Evaluation of the freezing–thawing effect in sand–silt mixtures using elastic waves and electrical resistivity [J]. Cold Regions Science and Technology, 2015, 113: 1−11.

[20] WANG T L, LIU Y J, YAN H, XU L. An experimental study on the mechanical properties of silty soils under repeated freeze–thaw cycles [J]. Cold Regions Science and Technology, 2015, 112: 51−65.

[21] ROUSTAEI M, ESLAMI A, GHAZAVI M. Effects of freeze–thaw cycles on a fiber reinforced fine grained soil in relation to geotechnical parameters [J]. Cold Regions Science and Technology, 2015, 120: 127−137.

[22] XU X, DONG Y, FAN C. Laboratory investigation on energy dissipation and damage characteristics of frozen loess during deformation process [J]. Cold Regions Science and Technology, 2015, 109: 1−8.

[23] JAMSHIDI R, LAKE C B. Hydraulic and strength performance of three cement-stabilized soils subjected to cycles of freezing and thawing [J]. Canadian Geotechnical Journal, 2015, 52(3): 283−294.

[24] JAMSHIDI R J, LAKE C B, GUNNING P, HILLS C D. Effect of freeze/thaw cycles on the performance and microstructure of cement-treated soils [J]. Journal of Materials in Civil Engineering, 2016, 28(12): 04016162.

[25] ROSA M G, CETIN B, EDIL T B, BENSON C H. Freeze–thaw performance of fly ash–stabilized materials and recycled pavement materials [J]. Journal of Materials in Civil Engineering, 2017, 29(6): 04017015.

[26] GEER S, BERGER J R, PARNELL W J, MUSTOE G G W. A comparison of discrete element and micromechanical methods for determining the effective elastic properties of geomaterials [J]. Computers and Geotechnics, 2017, 87: 1−9.

[27] MCROBERTS E C, MORGENSTERN N R. The stability of thawing slopes [J]. Canadian Geotechnical Journal, 1974, 11(4): 447−469.

[28] SRIVASTAVA P K, CHANDEL C, MAHAJAN P, PANKAJ P. Prediction of anisotropic elastic properties of snow from its microstructure [J]. Cold Regions Science and Technology, 2016, 125: 85−100.

[29] HUANG F, ZHANG M, WANG F, LING T H, YANG X L. The failure mechanism of surrounding rock around an existing shield tunnel induced by an adjacent excavation [J]. Computers and Geotechnics, 2020, 117: 103236.

[30] LIU E L, LUO K T, ZHANG S Y. Binary medium model for structured soils with initial stress-induced anisotropy [J]. Rock and Soil Mechanics, 2013, 34(11): 3103−3109.

[31] ZHOU Z, LI F, YANG H, GAO W, MIAO L. Orthogonal experimental study of soil–rock mixtures under the freeze–thaw cycle environment [J]. International Journal of Pavement Engineering, 2019: 1−13. DOI: https://doi.org/10.1080/10298436.2019.1686634.

[32] SHENG D, ZHANG S, YU Z, ZHANG J. Assessing frost susceptibility of soils using PCHeave [J]. Cold Regions Science and Technology, 2013, 95: 27−38.

[33] ZHOU Z, YANG H, WANG X C, LIU B C. Model development and experimental verification for permeability coefficient of soil-rock mixture [J]. International Journal of Geomechanics, 2016, 17(4): 04016106.

[34] CHEN X, TANG C A, YU J, ZHOU J F, CAI Y Y. Experimental investigation on deformation characteristics and permeability evolution of rock under confining pressure unloading conditions [J]. Journal of Central South University, 2018, 25(8): 1987−2001.

[35] ZHANG H Y, XU W J, YU Y Z. Numerical analysis of soil-rock mixture's meso-mechanics based on biaxial test [J]. Journal of Central South University, 2016, 23(3): 685−700.
[36] ZHOU Z, GAO W Y, LIU Z Z, ZHANG C C. Influence zone division and risk assessment of underwater tunnel adjacent constructions [J]. Mathematical Problems in Engineering, 2019, 3: 1−10.
[37] THOMAS H R, CLEALL P J, LI Y, HARRIS C, KERN-LUETSCHG M. Modelling of cryogenic processes in permafrost and seasonally frozen soils [J]. Géotechnique, 2009, 59(3): 173−184.

(Edited by YANG Hua)

中文导读

不同围压下土石混合体的弹性模量冻融损伤机理

摘要：土石混合体作为路基填料的常用材料，常处于冻融循环和不同围压的环境中。为了研究不同围压下土石混合体弹性模量的冻融损伤机理，提出了土石混合体细观界面冻融损伤系数的概念，研究了冻融循环环境对土石混合体的细观界面破坏现象，继而提出了针对冻融损伤下土石混合体弹性模量计算的双包体嵌入式冻融损伤模型。然后，利用正交试验，围绕不同围压下 5 个主要影响因素(含石量、压实度、冻融次数、含水率、冻结温度)对冻融循环环境下土石混合体静力学特性的影响进行了一系列大型三轴试验。通过对试验结果的分析，得到围压和试验因素对土石混合体弹性模量的影响规律，验证了双包体嵌入模型预测冻融循环环境下土石混合体弹性模量的准确性。实验结果表明：随着围压的增加，土石混合体弹性模量近似线性增加；含石量和压实度是影响土石混合体弹性模量最关键的因素，含石量和压实度越大，弹性模量越大；随着冻融循环次数的增加，土石混合体细观结构界面冻融损伤系数和弹性模量减小。

关键词：土石混合体；冻融循环；围压；弹性模量；损伤系数